AGU PUBLICATIONS

Geophysical Research Letters

RESEARCH LETTER
10.1002/2017GL074767

Key Points:
- The 2017 Valparaíso sequence occurred between the two main patches of moment release from the 1985 Valparaíso earthquake
- A large gap in historic ruptures south of the 2017 sequence, suggests a potential for great-sized earthquakes here in the near future
- Low resolution in geodetic coupling to the south of the 2017 sequence denotes the need for seafloor geodetic monitoring in subduction zones

Supporting Information:
- Supporting Information S1

Correspondence to:
J. L. Nealy,
jnealy@usgs.gov

Citation:
Nealy, J. L., M. W. Herman, G. L. Moore, G. P. Hayes, H. M. Benz, E. A. Bergman, and S. E. Barrientos (2017), 2017 Valparaíso earthquake sequence and the megathrust patchwork of central Chile, *Geophys. Res. Lett.*, *44*, 8865–8872, doi:10.1002/2017GL074767.

Received 29 JUN 2017
Accepted 17 AUG 2017
Accepted article online 29 AUG 2017
Published online 14 SEP 2017

2017 Valparaíso earthquake sequence and the megathrust patchwork of central Chile

Jennifer L. Nealy[1], Matthew W. Herman[2], Ginevra L. Moore[1], Gavin P. Hayes[1], Harley M. Benz[1], Eric A. Bergman[3], and Sergio E. Barrientos[4]

[1]National Earthquake Information Center, U.S. Geological Survey, Golden, Colorado, USA, [2]Department of Geosciences, Pennsylvania State University, University Park, Pennsylvania, USA, [3]Global Seismological Services, Golden, Colorado, USA, [4]Centro Sismologico Nacional, Universidad de Chile, Santiago, Chile

Abstract In April 2017, a sequence of earthquakes offshore Valparaíso, Chile, raised concerns of a potential megathrust earthquake in the near future. The largest event in the 2017 sequence was a *M*6.9 on 24 April, seemingly colocated with the last great-sized earthquake in the region—a *M*8.0 in March 1985. The history of large earthquakes in this region shows significant variation in rupture size and extent, typically highlighted by a juxtaposition of large ruptures interspersed with smaller magnitude sequences. We show that the 2017 sequence ruptured an area between the two main slip patches during the 1985 earthquake, rerupturing a patch that had previously slipped during the October 1973 *M*6.5 earthquake sequence. A significant gap in historic ruptures exists directly to the south of the 2017 sequence, with large enough moment deficit to host a great-sized earthquake in the near future, if it is locked.

1. Introduction

The Chilean subduction zone has hosted three great-sized earthquakes in the 21st century to date, two of which have occurred in central Chile—a *M*8.8 in February 2010 offshore the Maule region and a *M*8.3 in September 2015 offshore of Illapel. In April 2017, an intense seismic sequence off the coast near Valparaíso (between the Maule and Illapel ruptures) drew further attention to this active subduction zone. The sequence, which occurred in the same region as the 1985 *M*8.0 earthquake, began on 22 April 2017 and was punctuated by events of *M*6.0 on 23 April, *M*6.9 on 24 April, and *M*5.9 on 28 April, before tapering off in early May. In all, the Centro Sismologico Nacional (CSN) recorded over 600 *M*2.5+ earthquakes over a 2 week period. Given the location of this sequence, the 2017 events raise questions about the potential seismic hazard for another large earthquake in the near future. Thus, the 2017 Valparaíso sequence provides us with an opportunity to consider a smaller earthquake in the context of previous great-sized earthquakes in a region with variability in regard to the spatial and temporal evolution of seismicity.

Spatially, the setting of the Valparaíso sequence is also of interest because it occurs adjacent to a suggested segment boundary. The ruptures of both the 1985 Valparaíso and the 2015 Illapel events were bounded at ~32–33° (respectively, to the north of the 1985 event and south of the 2015 event; Figure 1). Here the Juan Fernandez Ridge enters the subduction trench, partitioning the subduction zone into a flat slab region to the north and a steeper dipping portion to the south. It is possible that this bathymetric feature marks a long-term segment boundary of the Chilean subduction zone [*Pardo et al.*, 2002; *Yáñez et al.*, 2002].

The temporal evolution of the 2017 Valparaíso events is of interest due to the variable nature of previous great-sized earthquake sequences. The 2010 *M*8.8 Maule earthquake that ruptured the plate boundary directly to the south of the Valparaíso events, and the 2015 *M*8.3 Illapel earthquake directly to the north, had no foreshock activity. In contrast, the 1985 *M*8.0 earthquake that ruptured the same portion of the plate boundary as the Valparaíso earthquakes had a pronounced foreshock sequence, with several moderate-to-large earthquakes migrating toward the 1985 main shock over the preceding 15 years [*Korrat and Madariaga*, 1986], and a cluster of foreshocks occurring over the 10 days prior to the main shock [*Comte et al.*, 1986].

We can gain insight into the Valparaíso sequence by evaluating results from finite fault modeling, relative and absolute relocation of the sequence, moment tensor computation, and Coulomb stress, and moment deficit analyses. This suite of information can tell us more about the nature of the sequence, its seismotectonic context relative to previous great earthquakes in the region, and the future seismic hazard in this portion of the Chilean subduction zone.

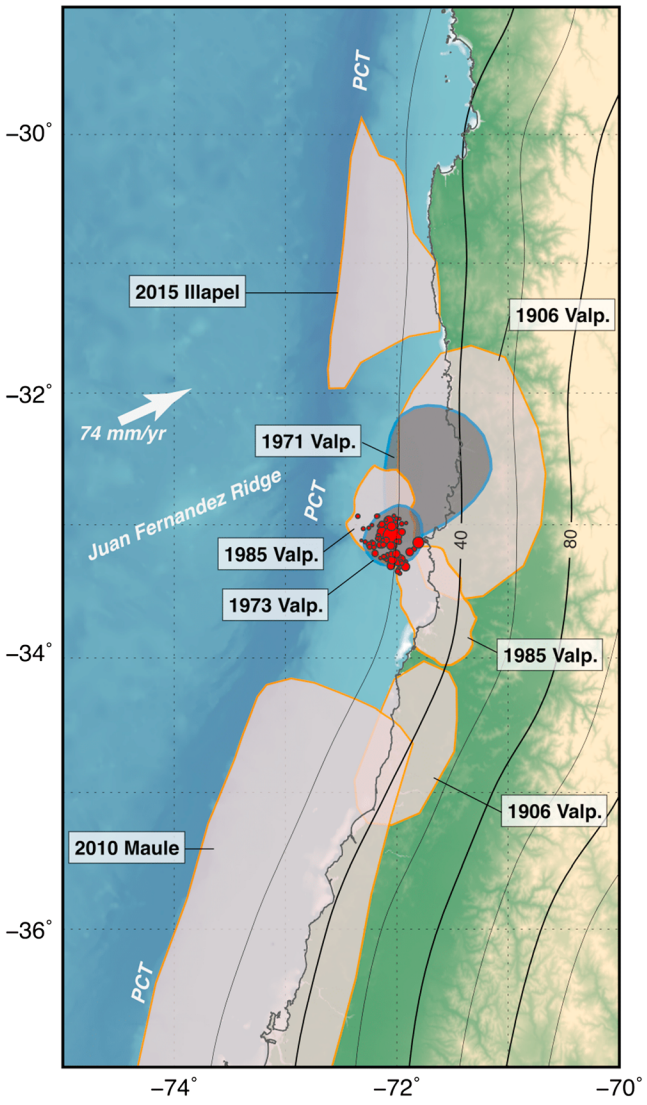

Figure 1. Seismotectonic context of large 20th and 21st century earthquakes in central Chile. Light gray polygons describe rupture areas of great-sized events (1906 *M*8.4–8.6 from F. del Campo, personal communication, 2017 (see supporting information for further details); 1985 *M*8.0, from *Barrientos* [1997]; 2010 *M*8.8 from *Hayes et al*. [2013]; 2015 *M*8.3 from *Hayes* [2017]). Dark gray polygons are the aftershock zones of the 1971 *M*7.8, and the 1973 *M*6.5 earthquake sequences (digitized from *Korrat and Madariaga* [1986]). Red circles are the relocated epicenters of the 2017 sequence. PCT indicates the location of the Peru-Chile Trench. See Figure S1 for additional details, including background seismicity.

2. Historic Seismicity

The coast of central Chile (29°S to 37°S) is one of the most seismically active areas on Earth and has hosted 15 great-sized ($M \geq 8.0$) earthquakes over the past four and a half centuries (Figure S1 in the supporting information). Prior to the twentieth century, there were eight great-sized earthquakes; these are detailed in the supplement. During the twentieth century, there were five great-sized earthquakes along the central Chilean coast. In 1906, a *M*8.4–8.6 event occurred off the coast of Valparaíso on 16 August. This earthquake is thought to be collocated with the *M*8–8.5 1822 earthquake and the 1985 *M*8.0 Valparaíso earthquake [*Okal*, 2005] and ruptured ~400 km of the plate boundary [*Beck et al*., 1998]. On 11 November 1922, a *M*8.3–8.4 event occurred off the coast of Huasco (~28.6°S), rupturing ~450 km of the northern subduction zone in this region, and was followed by extensive aftershocks. A *M*8–8.4 earthquake with an epicenter near Putu (~35.2°S) occurred on 1 December 1928, rupturing over ~100–150 km and causing damage from Valparaíso to Concepción [*Beck et al*., 1998; *Lomnitz*, 2004]. Near Illapel (~31.6°S), a *M*8.3 event on 6 April 1943 caused a minor local tsunami at Los Vilos and ruptured the plate interface between the 1906 and 1922 events (~200–250 km). Although not a great-sized earthquake, the 9 July 1971, *M*7.8 event is of interest due to the location of its rupture area, which is located predominantly to the north and downdip of the northern portion of the 1985 rupture area. The southward propagation of the 1971 earthquake was thought to have been impeded by a barrier that later failed and initiated the 1985 earthquake [*Korrat and Madariaga*, 1986].

The first great-sized Chilean earthquake that could be studied using broadband waveforms recorded by the Global Digital Seismograph Network was the 3 March 1985, *M*8.0 earthquake that occurred near Valparaíso [*Choy and Dewey*, 1988]. The 1985 event was found to have had a complex initiation, made up of two subevents with similar hypocenter locations [*Comte et al*., 1986]. The rupture of the 1985 earthquake propagated ~60 km to the north and ~110 km to the south, in an area previously ruptured in 1906, 1822, and 1730 [*Comte et al*., 1986; *Barrientos*, 1997].

Central Chile has also hosted two great-sized earthquakes in the beginning of the 21st century. On 27 February 2010, a *M*8.8 earthquake occurred off the coast of Maule (~35.5°S) [*Vigny et al*., 2011]. The Maule

earthquake had an active aftershock sequence with over 2500 *M*4+ aftershocks occurring over the 18 months following the main shock [*Hayes et al.*, 2013]. The northern limit of the area ruptured by the 2010 Maule earthquake abuts the approximate southern extents of the 1985 and 1906 earthquakes. The portion of the subduction zone extending ~150 km south of the 2010 hypocenter had last coseismically slipped in the 1835 earthquake [*Hayes et al.*, 2013]. The most recent great-sized Chilean earthquake was the 16 September 2015, *M*8.3 Illapel earthquake [*Melgar et al.*, 2016]. This event occurred over parts of the subduction zone last ruptured by the 1943, 1880, 1822, and 1730 earthquakes, and its rupture zone is approximately collocated with the 1880 and 1943 ruptures [*Herman et al.*, 2017], between 30°S and 33°S.

Historically, large earthquakes have not ruptured across 30°S where the Challenger Fracture Zone enters the trench; this feature is thought to act as a barrier to coseismic rupture [*Carena*, 2011; *Métois et al.*, 2012]. At ~32.5°S, the Juan Fernandez Ridge enters the trench and may have acted as a partial barrier to slip propagation in the 2015 Illapel event [*Barnhart et al.*, 2016]. The subducted Juan Fernandez Ridge is located at the southern edge of the flat slab segment (Figure S2) of the central Chile subduction zone from ~28°S to ~32°S. To the south of the Juan Fernandez Ridge, the Nazca plate subducts beneath the South America plate with a steeper dip, particularly evident at intermediate depths (Figure S2). The ridge is thus considered a segment boundary with low seismic activity [*Pardo et al.*, 2002; *Yáñez et al.*, 2002].

The 24 April 2017, *M*6.9 Valparaíso earthquake took place south of the Juan Fernandez Ridge, at ~33.1°S (Figure 1). This event occurred within the rupture area of the 1985 *M*8.0 Valparaíso earthquake in a region with a great-sized earthquake recurrence rate of 83 ± 9 years [*Comte et al.*, 1986]. The 2017 sequence began on 22 April with several small events ($M < 5$) culminating in a *M*6.0 earthquake the following day. An aftershock sequence of 10 earthquakes followed, with magnitudes ranging from *M*3.9 to *M*5.6. The aftershock sequence of the *M*6.0 event lasted approximately 28 h before the *M*6.9 earthquake at 21:38:26 UTC on 24 April. The aftershock sequence of the *M*6.9 event consisted of 101 *M*3.5+ aftershocks, the largest (*M*5.9) of which occurred on 28 April at 15:30:05 UTC.

3. Finite Fault Modeling, Calibrated Relocations, and Regional Moment Tensor Analysis

To better compare the 2017 Valparaíso earthquake with the previous great-sized earthquakes in the region, we first determine the distribution of main shock slip using a finite fault model (FFM) analysis of the rupture [*Ji et al.*, 2002]. The FFM inverts displacement records from 60 broadband *P* waveforms, 31 broadband *SH* waveforms, and 48 long-period surface waves. The Valparaíso main shock is at the limit of resolution for teleseismic FFMs, so velocity data were also incorporated to improve resolution. Our finite fault solution shows slip on the downdip portion of the inverted fault plane with peak slip of ~1 m to the southeast of the hypocenter. Our model produces synthetic surface displacements (assuming an elastic half-space) in good agreement with the two available GPS stations in the region (Table S1). For more details on the FFM see the provided link in section 7.

Barrientos [1997] examined coseismic slip for the 1985 Valparaíso earthquake by determining the slip distribution of the rupture region using leveling data, gravity measurements, mareograph data, tilt records, and tide gauge measurements. The resultant slip model shows maximum slip of ~4 m occurring in a southern slip lobe downdip of the 1985 main shock. A northern lobe of slip northwest and updip of the main shock has maximum slip of ~2.6 m. While offshore fault slip is difficult to recover in any geodetic inversion, and thus, the northern patch of slip in this model probably has higher uncertainty, the two-lobed pattern is dictated by the data; to reproduce observed subsidence in Valparaíso, slip must occur offshore (northern patch), and to reproduce observed landward tilting of the Rapel Lake basin, slip must take place downdip near Rapel Lake (southern patch). Slip during the 2017 Valparaíso earthquake lies in the saddle between these two 1985 slip lobes (Figures 2 and S3). The downdip cluster of aftershocks from the 2017 sequence is also located within this saddle, collocated with the foreshocks of the 1985 event. The 1985 foreshocks and 2017 aftershocks form a NE-SW line delineating the southeastern limit of the 2017 seismicity.

The location of the slip in the 2017 earthquake is generally anticorrelated with the foreshock and aftershock locations obtained using a multiple-event relocation method based on the hypocentroidal decomposition (HD) algorithm [*Jordan and Sverdrup*, 1981] and optimized to obtain calibrated locations, i.e., minimally biased locations with realistic estimates of uncertainty. The same technique was used to obtain improved

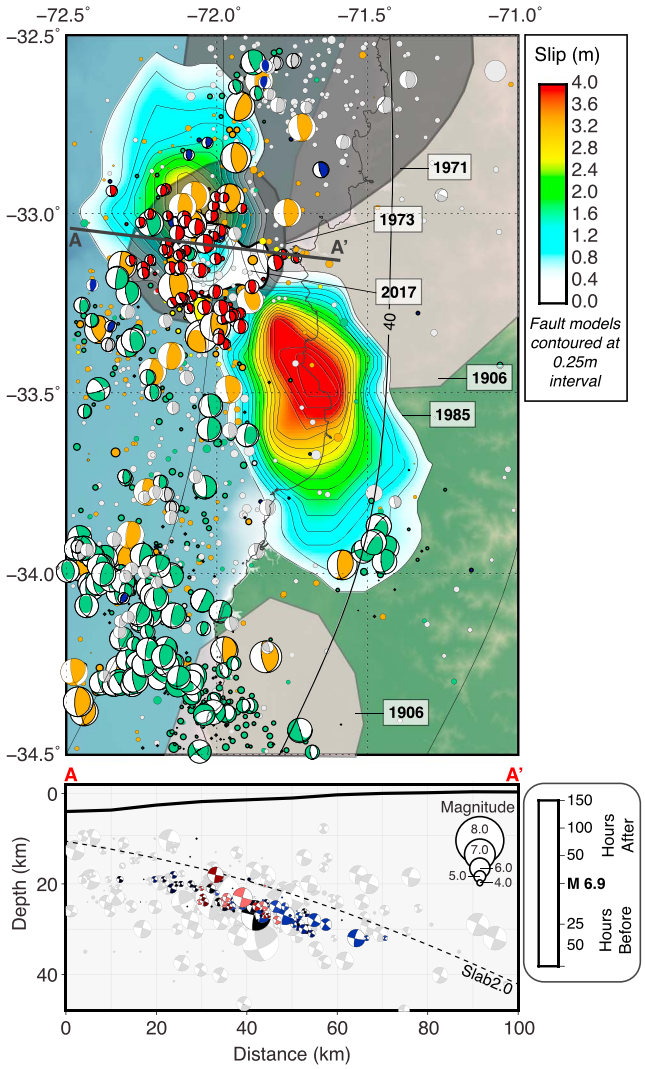

Figure 2. Finite fault models for the 1985 and 2017 Valparaíso earthquakes. The two-lobed model in the background is the slip model for the 1985 event from *Barrientos* [1997]. The smaller model between the two lobes of the 1985 model, outlined with a thick black line, is for the 2017 Valparaíso earthquake. The dark gray polygons show the aftershock areas of the 1971 *M*7.8 and 1973 *M*6.5 earthquakes. Orange focal mechanisms correspond to aftershocks of the 1985 Valparaíso earthquake; yellow are 1985 foreshocks; green are 2010 Maule aftershocks; blue relate to the 2015 Illapel event; red are the 2017 sequence; gray are background seismicity. The cross section (black line on the map) shows the depths of the 2017 Valparaíso sequence compared to the regional slab model [*Hayes et al.*, 2012; *Moore et al.*, 2017]. Valparaíso events with focal mechanisms are shown colored by time in relation to the main shock. Preliminary Determination of Epicenters (PDE) events with focal mechanisms up until 20 April 2017 are shown in gray. See Figure S3 for additional details including background seismicity.

locations for the 1985 Valparaíso sequence (Figure S4). The Valparaíso events were calibrated by relocating them together with nearby events from the 2010 Maule sequence for which there are arrival time readings at short epicentral distances from the temporary seismograph network deployed soon after that event [*Beck et al.*, 2014]. The hypocentroid (which establishes the absolute location of all events) of the Valparaíso cluster was calibrated using only data at less than 1.0° epicentral distance to minimize the biasing effect of poorly known velocity structure. The hypocentroid has an uncertainty of 1.4 km, and the uncertainty of individual epicenters of the 2017 sequence range from 2 to 5 km with the majority of epicenters (92%) having an uncertainty of less than 4 km. The average uncertainty in depth is ±4.1 km. All of the events in the 2017 Valparaíso foreshock-aftershock sequence surround the slip patch, while the events occurring on 28–30 April surround the southern and downdip edges of slip (Figure 2).

Regional moment tensors [*Herrmann et al.*, 2011] were produced for over half of the events in the 2017 Valparaíso sequence, allowing us to evaluate the relative distribution of upper plate, lower plate, and interface events. Regional moment tensor depths are all within the uncertainty estimates obtained from the HD relocations and had uncertainties in depth during modeling of <5 km, giving us confidence in their locations with respect to the slab. Most events in the sequence have moment tensors consistent with thrust faulting and are inferred to involve interplate slip. Four lower plate events occurred later in the aftershock sequence, along the southern updown and downdip edges of slip. No upper plate faulting appears to have been involved in the sequence.

4. Coulomb Stress Modeling

We compute Coulomb failure stress changes (ΔCFS) [*Reasenberg and Simpson*, 1992] throughout to evaluate the evolution of stress during the sequence, applying the approach of *Herman et al.* [2016] to determine

whether the sequence can be interpreted as a cascade of sequentially triggered events. Of the 54 relocated events with moment tensor solutions, 34 (63%) were positively loaded at their hypocenters by the preceding events (ΔCFS $>$ 0.01 MPa), 18 (33%) were negatively loaded (ΔCFS $<$ $-$0.01 MPa), and two (4%) were negligibly loaded (Figure S5). We also compare the percentage of positively loaded events during this sequence to the percent of positively loaded historical events (1994–2017; events from the Global Centroid Moment Tensor Catalog) [*Ekström et al.*, 2012]. Of the 17 historical events in the same region as the Valparaíso sequence, ~65% were positively loaded, ~23% were negatively loaded, and ~12% were negligibly loaded. Although the historical earthquakes appear to be positively loaded at a higher rate than the events in the 2017 sequence, there are not enough events to generate robust statistics, and stress changes from the historical large earthquakes in the region may also affect the location of these events. This analysis suggests that there is no clear evidence for the Valparaíso sequence being a series of sequentially triggered events responding to cascading ΔCFS.

By considering the stress changes from the 1971, 1985, 2010, and 2015 earthquakes, along with 46 years of interseismic loading, we can estimate the historical contribution of each on the loading at the location of the 2017 sequence. We use the finite fault models from the Maule and Illapel earthquakes [*Hayes*, 2017], the *Barrientos* [1997] model for the 1985 Valparaíso earthquake, and a rupture polygon (assuming a uniform 0.5 m of slip) for the 1971 Valparaíso earthquake. Stress changes from interseismic loading are estimated by putting back slip onto Slab1.0 at seismogenic depths [*Hayes et al.*, 2012]. Combined, the interseismic loading and four previous events add ~4–5 MPa of ΔCFS to the location of the 2017 Valparaíso sequence. The majority of this additional ΔCFS comes from the interseismic loading (~4 MPa on average). The 1971 and 1985 events reduce the ΔCFS loading at the 2017 sequence by ~0.3 MPa. The ΔCFS of the region is slightly increased by incorporating the Maule and Illapel events, which contribute ~0.1–0.2 MPa. In addition, the stress drop for the 2017 Valparaíso earthquake is on the same order of magnitude as the stress increase due to interseismic loading. The magnitude of the stress drop of the 2017 event coupled with the Coulomb stress history of the region suggests that despite the previous large events surrounding the 2017 sequence, this area can still be considered a seismic gap.

5. Discussion

Combining the results from the relocations, regional moment tensor analysis, finite fault modeling, and Coulomb failure stress analysis, we can draw comparisons between the Valparaíso sequence and recent large sequences in the region. We can also consider how the four most recent historic earthquakes loaded the area that ruptured in the 2017 sequence and analyze the moment deficit remaining in the region.

The 2014 *M*8.2 Iquique earthquake (in northern Chile) had an active foreshock sequence with a clear pattern of migration of events leading up to the main shock. Similarly, the locations of our relocated 2017 events show a broad southward migration with time (Figure S6). Coulomb failure stress analysis of the Iquique sequence indicates that its migration was driven by cascading ΔCFS, ultimately leading to the main shock. Results are less clear for the 2017 Valparaíso sequence, likely because of the smaller size and limited spatial footprint of the events. In contrast, neither the 2010 Maule nor the 2015 Illapel earthquakes had any foreshock activity. Regional moment tensor analysis of the Valparaíso events shows that the majority of earthquakes in the sequence were interface earthquakes. No upper plate faulting occurred, and there was minimal lower plate faulting. In this the Valparaíso sequence echoes the Iquique and Illapel sequences, which also elicited little to no upper plate response (though the Iquique sequence began with a large upper plate event). In contrast, the 2010 Maule earthquake ruptured most of the seismogenic zone and its aftershock sequence contained mechanisms spanning a broad range of the faulting spectrum [*Hayes et al.*, 2014]. From these comparisons, we conclude that the 2017 Valparaíso sequence more closely resembles the 2014 Iquique sequence than the Illapel or Maule sequences. Unlike Iquique, of course, the 2017 sequence did not culminate in a great-sized earthquake (or has not, as of the middle of August 2017).

From a Coulomb stress analysis of the region, we are able to evaluate the contributions of the four previous large events to the loading of the region hosting the 2017 sequence. The 2017 sequence occurred between the Maule and Illapel events in a section of the subduction zone last ruptured by the 1985 and 1971 Valparaíso earthquakes. The 2017 sequence was in a region that experienced positive loading with a ΔCFS

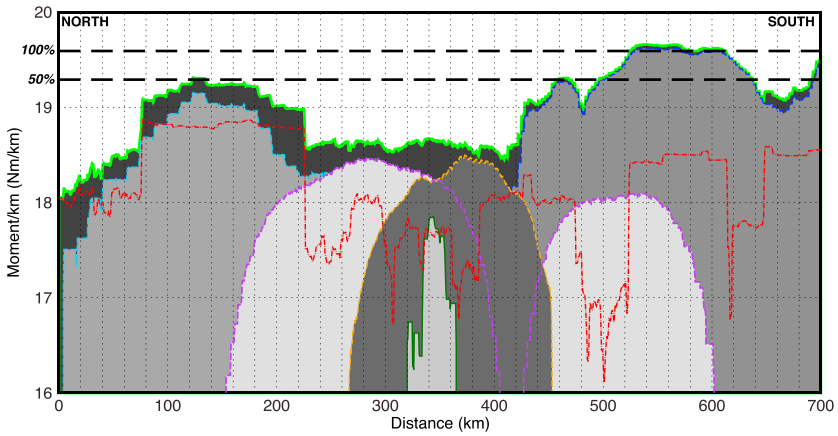

Figure 3. Moment deficit along the strike of the subduction zone in central Chile. Moment calculated for historical seismicity from the USGS Combined Catalog since 1900, resolved as moment per kilometer along strike. For each earthquake, moment is divided evenly over the length of the rupture, calculated using empirical relations [*Allen and Hayes*, 2017]. For the largest earthquakes (*M*8+), more accurate rupture areas are used (Figure 1). The 2015 Illapel earthquake is shown in light blue. The 2010 Maule earthquake is shown in dark blue. The 1906, 1985, and 2017 Valparaíso earthquakes are shown in purple, orange, and dark green, respectively. The red line shows moment from background seismicity. Green represents all summed moment. The two horizontal black dashed lines represent moment accumulation since 1900 given 100% (top) and 50% (bottom) coupling.

between 0.04 and 0.1 MPa (Figure S7). We varied the modeling parameters of the Coulomb stress analysis to explore the robustness of this result and found that there is positive loading regardless of the parameters chosen. Evaluating the individual Coulomb stress contributions of the previous four earthquakes and interseismic loading, we determine that the majority of additional Coulomb stress is contributed by incorporating 46 years of interseismic loading. We conclude, therefore, that the 2017 sequence is located in an effective "seismic gap" despite the previous large events in the surrounding region.

Comparing the 2017 Valparaíso earthquakes to the 1985 Valparaíso sequence indicates that the recent events occurred in the "saddle" (slip minima) between the two patches of moment release from the 1985 main shock (Figure 2). The HD locations of the 1985 sequence show that its foreshocks also fell between the two lobes of slip and lie at the southeastern limit of the 2017 seismicity. A *M*7.8 earthquake in 1971 ruptured much of the seismogenic zone downdip of the northern patch of 1985 slip (Figures 2 and 3). The region containing the 2017 sequence has markedly low background seismicity and also slipped during a swarm-like sequence of events following a *M*6.5 earthquake in October 1973 [*Korrat and Madariaga*, 1986]. This "barrier" was subsequently breached in 1985, but with low slip, facilitating its isolated rerupture in 2017. We postulate that the subduction zone patch ruptured in 2017 is thus somewhat isolated from the surrounding subduction zone but responds to—and, importantly, helps modulate—stress transfer between and strain release on adjacent sections of the megathrust.

The collection of historic ruptures in central Chile reveals a patchwork pattern of megathrust slip over the 20th and early 21st century. The largest rupture zones in particular abut one another rather than demonstrate any evidence for asperity rerupture. At least with regard to the two most recent large events near Valparaíso in 1906 and 1985, this suggests that the return period of great-sized earthquakes in the region of 83 ± 9 years from *Comte et al.* [1986] may not be reflective of truly repeating earthquake processes. The smaller sequences (1971, 1973, and 2017 events) appear to spatially complement the larger ruptures, breaking smaller patches surrounding those larger events. The 2017 sequence may represent the first clear evidence of rerupture in this region over this time frame, having broken a portion of the megathrust that slipped in a moderate-sized event in 1973, and to a lesser extent during the 1985 *M*8.0 earthquake.

The remaining patches (those parts of the megathrust that have not ruptured over the same time period) would thus logically be where one would expect future earthquakes to occur. Analysis of moment accumulation and release along the margin since the turn of the twentieth century (Figure 3) shows that the 2017 sequence coincides with a depression in the moment release from the 1985 event (orange line), near the

southern edge of the main slip patch of the 1906 event (purple line). Total moment (green line) shows a potential slip deficit remains in this region; over a length of ~300 km between the Illapel and Maule events, enough strain is stored for a M ~ 8.5+ event, if the seismogenic zone is fully coupled. While geodetic coupling models [e.g., *Métois et al.*, 2012] suggest low coupling over much of the region south of the Valparaíso sequence, particularly in the shallow subduction zone (Figure S8), resolution in such models is low in the near-trench region. As such, we cannot rule out the possibility of a future large to great-sized event here, involving slip over the shallow gap in large ruptures (Figures 1 and S8). Any such shallow rupture could also be accompanied by a significant tsunami. North of the Juan Fernandez Ridge, an area of high coupling coincides with a gap between the southern edge of the 2015 Illapel earthquake and the northern and updip edges of the 1985 and 1906 events, respectively (Figure S8). The moment deficit here is sufficient for an earthquake as large as ~M7.8–8.2, depending on the area of slip and amount of coupling. We note that these calculations are based on the assumption that moment deficit was effectively zero at the beginning of the twentieth century, which is unlikely to be the case. Any pre-1900 strain accumulation (e.g., since the 1822 M8.0–8.5 or 1730 M8.5–9.0 earthquakes; Figure S1) would act to increase the size of potential future earthquakes in the regions analyzed here.

6. Conclusions

With a variety of tools, we have assessed the seismotectonic setting of the 2017 Valparaíso earthquake sequence, placing it into the context of historic ruptures in the region. This sequence, which began on 22 April 2017, was punctuated by a M6.9 rupture on 24 April, and ended in early May 2017, was confined to a small area in a region of low slip between the two major asperities of the 1985 M8.0 Valparaíso earthquake. The southern extent of 2017 seismicity coincides with the 10 day foreshock sequence of the 1985 event, and the entire 2017 sequence defines an area that also hosted a similar sequence of earthquakes in 1973, punctuated by a M6.5 event. Foreshocks and aftershocks of the 2017 M6.9 event surround the main slip patch of this large earthquake, as has been observed in a number of recent megathrust earthquake sequences.

The compilation of historic ruptures in this region reveals a pattern of complementary slip on the megathrust, rather than one of repeating events. With the exception of the small patch ruptured in 1973 and again in 2017 (with minor slip during the 1985 earthquake as well), no other part of the megathrust between 32°S and 34°S has reruptured with significant slip. A large gap in historic ruptures remains to the south of the 2017 sequence and updip of 1985 and 1906 ruptures; while geodetic coupling models suggest this section of the megathrust is not locked, their lack of resolution near the oceanic trench means that we cannot rule out the possibility of a great-sized earthquake in this region. Hazard for a large-to-great-sized event also remains farther north, between the northern edge of the 1985 event and the southern edge of the 2015 Illapel earthquake, and adjacent to where the Juan Fernandez Ridge enters the subduction zone. This ridge seems to have played a role in limiting the along-strike extent of earthquake rupture in the past, so any future earthquake here may also be limited by this geometrical feature.

Regardless of whether the 2017 Valparaíso sequence represents foreshock activity of a future larger event, careful analysis of sequences like this helps to increase our understanding of the behavior of the megathrust in this region. Comparing the Valparaíso sequence to historic earthquakes provides us with more insight into a subduction zone with significant variability in the spatiotemporal evolution of seismicity. Our observations provide context for why this sequence occurred where it did, and in turn help improve our ability to rapidly respond to megathrust events—an important task considering that potential remains for this region to host a great earthquake in the near future. The lack of resolution in geodetic coupling in near-trench regions of subduction zones, coupled with the associated high (and increased) hazard offshore Valparaíso, is a strong argument for the need for seafloor geodetic monitoring to better resolve the potential for future megathrust ruptures.

7. Data and Resources

Data used in this article are available through the U.S. Geological Survey (USGS) and the CSN. The finite fault solution for the 2017 Valparaíso sequence can be found online at https://earthquake.usgs.gov/earthquakes/eventpage/us10008kce#finite-fault. Figures were produced using the Generic Mapping Tools software package [*Wessel and Smith*, 1991]. Bathymetry for basemaps uses Gebco2014 (http://www.gebco.net, last accessed April 2017). The catalog for the 2017 Valparaíso sequence is available in Science Base (doi:10.5066/F71Z439C).

References

Allen, T. I., and G. P. Hayes (2017), Alternative rupture-scaling relationships for subduction interface and other offshore environments, *Bull. Seismol. Soc. Am.*, *107*(3), 1240–1253, doi:10.1785/0120160255.

Barnhart, W. D., J. R. Murray, R. W. Briggs, F. Gomez, C. P. Miles, J. Svarc, S. Riquelme, and B. J. Stressler (2016), Coseismic slip and early afterslip of the 2015 Illapel, Chile, earthquake: Implications for frictional heterogeneity and coastal uplift, *J. Geophys. Res. Solid Earth*, *121*, 6172–6191, doi:10.1002/2016JB013124.

Barrientos, S. E. (1988), Slip distribution of the 1985 Central Chile earthquake, *Tectonophysics*, *145*, 225–241.

Barrientos, S. E. (1997), Central Chile: An example of quasi-static crustal behavior, *Island Arc*, *6*(3), 281–287, doi:10.1111/j.1440-1738.1997.tb00178.x.

Beck, S., S. Barrientos, E. Kausel, and M. Reyes (1998), Source characteristics of historic earthquakes along the central Chile subduction zone, *J. South Am. Earth Sci.*, *11*(2), 115–129, doi:10.1016/S0895-9811(98)00005-4.

Beck, S., A. Rietbrock, F. Tilmann, S. Barrientos, A. Meltzer, O. Oncken, K. Bataille, S. Roecker, J. P. Vilotte, and R. M. Russo (2014), Advancing subduction zone science after a big quake, *Eos*, *95*(23), 193–194, doi:10.1002/2014EO230001.

Carena, S. (2011), Subducting-plate topography and nucleation of great and giant earthquakes along the South American trench, *Seismol. Res. Lett.*, *82*(5), 629–637, doi:10.1785/gssrl.82.5.629.

Carvajal, M., M. Cisternas, and P. A. Catalán (2017), Source of the 1730 Chilean earthquake from historical records: Implications for the future tsunami hazard on the coast of Metropolitan Chile, *J. Geophys. Res. Solid Earth*, *122*, 3648–3660, doi:10.1002/2017JB014063.

Choy, G. L., and J. W. Dewey (1988), Rupture process of an extended earthquake sequence: Teleseismic analysis of the Chilean earthquake of March 3, 1985, *J. Geophys. Res.*, *93*(B2), 1103–1118, doi:10.1029/JB093iB02p01103.

Comte, D., A. Eisenberg, E. Lorca, M. Pardo, L. Ponce, R. Saragoni, S. K. Singh, and G. Suárez (1986), The 1985 central Chile earthquake: A repeat of previous great earthquakes in the region?, *Science(Washington)*, *233*(4762), 449–453.

Ekström, G., M. Nettles, and A. M. Dziewoński (2012), The global CMT project 2004–2010: Centroid-moment tensors for 13,017 earthquakes, *Phys. Earth Planet. Inter.*, *200-201*, 1–9, doi:10.1016/j.pepi.2012.04.002.

Hayes, G. P. (2017), The finite, kinematic rupture properties of great-sized earthquakes since 1990, *Earth Planet. Sci. Lett.*, *468*, 94–100, doi:10.1016/j.epsl.2017.04.003.

Hayes, G. P., E. Bergman, K. L. Johnson, H. M. Benz, L. Brown, and A. S. Meltzer (2013), Seismotectonic framework of the 2010 February 27 M_w 8.8 Maule, Chile earthquake sequence, *Geophys. J. Int.*, *195*(2), 1034–1051, doi:10.1093/gji/ggt238.

Hayes, G. P., M. W. Herman, W. D. Barnhart, K. P. Furlong, S. Riquelme, H. M. Benz, E. Bergman, S. Barrientos, P. S. Earle, and S. Samsonov (2014), Continuing megathrust earthquake potential in Chile after the 2014 Iquique earthquake, *Nature*, *512*, 295–298, doi:10.1038/nature13677.

Hayes, G. P., D. J. Wald, and R. L. Johnson (2012), Slab1.0: A three-dimensional model of global subduction zone geometries, *J. Geophys. Res.*, *117*, B01302, doi:10.1029/2011JB008524.

Herman, M. W., K. P. Furlong, G. P. Hayes, and H. M. Benz (2016), Foreshock triggering of the 1 April 2014 M_w 8.2 Iquique, Chile, earthquake, *Earth Planet. Sci. Lett.*, *447*, 119–129, doi:10.1016/j.epsl.2016.04.020.

Herman, M. W., J. L. Nealy, W. L. Yeck, W. D. Barnhart, G. P. Hayes, K. P. Furlong, and H. M. Benz (2017), Integrated geophysical characteristics of the 2015 Illapel, Chile, earthquake, *J. Geophys. Res. Solid Earth*, *122*, 4691–4711, doi:10.1002/2016JB013617.

Herrmann, R. B., L. Malagnini, and I. Munafò (2011), Regional moment tensors of the 2009 L'Aquila earthquake sequence, *Bull. Seismol. Soc. Am.*, *101*(3), 975–993, doi:10.1785/0120100184.

Ji, C., D. J. Wald, and D. V. Helmberger (2002), Source description of the 1999 Hector mine, California, earthquake, Part I: Wavelet domain inversion theory and resolution analysis, *Bull. Seismol. Soc. Am.*, *92*(4), 1192–1207, doi:10.1785/0120000916.

Jordan, T. H., and K. A. Sverdrup (1981), Teleseismic location techniques and their application to earthquake clusters in the south-central Pacific, *Bull. Seismol. Soc. Am.*, *71*(4), 1105–1130.

Korrat, I., and R. Madariaga (1986), Rupture of the Valparaiso (Chile) gap from 1971 to 1985, in *Earthquake Source Mechanics*, edited by S. Das, J. Boatwright, and C. H. Scholz, pp. 247–258, AGU, Washington, D. C., doi:10.1029/GM037p0247

Lomnitz, C. (2004), Major earthquakes of Chile: A historical survey, 1535–1960, *Seismol. Res. Lett.*, *75*(3), 368–378, doi:10.1785/gssrl.75.3.368.

Melgar, D., W. Fan, S. Riquelme, J. Geng, C. Liang, M. Fuentes, G. Vargas, R. M. Allen, P. M. Shearer, and E. J. Fielding (2016), Slip segmentation and slow rupture to the trench during the 2015, M_w8. 3 Illapel, Chile earthquake, *Geophys. Res. Lett.*, *43*, 961–966, doi:10.1002/2015GL067369.

Métois, M., A. Socquet, and C. Vigny (2012), Interseismic coupling, segmentation and mechanical behavior of the central Chile subduction zone, *J. Geophys. Res.*, *117*, B03406, doi:10.1029/2011JB008736.

Moore, G. L., G. P. Hayes, D. E. Portner, M. Furtney, H. E. Flamme, and M. Hearne (2017), Slab2—Updated subduction zone geometries and modeling tools, In SSA Annual Meeting Abstracts.

Okal, E. A. (2005), A re-evaluation of the great Aleutian and Chilean earthquakes of 1906 August 17, *Geophys. J. Int.*, *161*(2), 268–282, doi:10.1111/j.1365-246X.2005.02582.x.

Pardo, M., D. Comte, and T. Monfret (2002), Seismotectonic and stress distribution in the central Chile subduction zone, *J. South Am. Earth Sci.*, *15*(1), 11–22, doi:10.1016/S0895-9811(02)00003-2.

Radiguet, M., F. Cotton, M. Vergnolle, M. Campillo, B. Valette, and V. Kostoglodov (2011), Spatial and temporal evolution of a long term slow slip event: The 2006 Guerrero slow slip event, *Geophys. J. Int.*, *184*, 816–828.

Reasenberg, P. A., and R. W. Simpson (1992), Response of regional seismicity to the static stress change produced by the Loma Prieta earthquake, *Science*, *255*(5052), 1687.

Steffen, H. (1907), *Contribuciones para un Estadio Científico del Terremoto del 16 de Agosto de 1906*, *Anales de la Universidad de Chile*, Santiago de Chile.

Tarantola, A., and B. Valette (1992), Inverse problems = quest for information, *J. Geophys.*, *50*, 159–170.

Udías, A., R. Madariaga, E. Buforn, D. Muñoz, and M. Ros (2012), The large Chilean historical earthquakes of 1647, 1657, 1730, and 1751 from contemporary documents, *Bull. Seismol. Soc. Am.*, *102*(4), 1639–1653, doi:10.1785/0120110289.

Vigny, C., et al. (2011), The 2010 M_w 8.8 Maule megathrust earthquake of Central Chile, monitored by GPS, *Science*, *332*(6036), 1417–1421, doi:10.1126/science.1204132.

Wessel, P., and W. H. Smith (1991), Free software helps map and display data, *Eos Trans. AGU*, *72*(41), 441–446, doi:10.1029/90EO00319.

Yáñez, G., J. Cembrano, M. Pardo, C. Ranero, and D. Selles (2002), The challenger–Juan Fernández–Maipo major tectonic transition of the Nazca–Andean subduction system at 33–34°S: Geodynamic evidence and implications, *J. South Am. Earth Sci.*, *15*(1), 23–38, doi:10.1016/S0895-9811(02)00004-4.